

Preparation and Ethanol Sensing Behavior of Spinel-type Nanosized Mixed Ferrites Containing Zn

V. D. KAPSE^{1,*}, F.C. RAGHUWANSHI², V.S. SANGAWAR³

¹ Department of Physics, Arts, Science and Commerce College, Chikhaldara 444807, Maharashtra, India

² Department of Physics, Vidyabharati Mahavidyalaya, Amravati 444602, Maharashtra, India

³ Department of Physics, Government Vidarbha Institute of Science & Humanities, Amravati 444604, Maharashtra, India, Corresponding author: vdk.nano@gmail.com

Abstract

Nanocrystalline $Ni_{1-x}Zn_xFe_2O_4$ ($x = 0, 0.2, 0.3$ and 0.4) mixed ferrite with cubic spinel structure was successfully prepared by the citrated sol-gel method followed by calcinations at $600^\circ C$. Characterization of the materials was performed by XRD. Indirect-heating sensors using as-prepared powders of mixed ferrite as sensitive materials were fabricated on an alumina tube with Au electrodes and Platinum wires. The gas response of $Ni_{1-x}Zn_xFe_2O_4$ based thick film sensor to C_2H_5OH , was measured. $Ni_{0.6}Zn_{0.4}Fe_2O_4$ based thick film sensor showed better response to ethanol gas at $300^\circ C$ as compared with other tested reducing gases. The observed gas sensing potential is explained by using the reducer nature of the gaseous species that react on the surface of the heated semi-conducting mixed oxide. The sensor exhibited a fast response and a good recovery.

Keywords: X-ray diffraction; Mixed ferrites; Gas sensor; Sensor response.

1. Introduction

Metal oxides based semiconductor gas sensors are commonly used in the monitoring of toxic pollutants and can provide the necessary sensitivity, selectivity and stability required by such systems [1]. Gas-sensing properties of semiconducting materials based on SnO_2 , ZnO , WO_3 , TiO_2 , In_2O_3 , Fe_2O_3 , mixed oxides, ferrites and complex metal oxides have been extensively studied to detect explosive, inflammable, toxic and hazardous gases. In the last decade there is growing interest to investigate the gas sensing properties of ferrites [2-4]. $NiFe_2O_4$ (AB_2O_4) is a well-known inverse spinel with all Ni^{2+} ions on the B-sites and Fe^{3+} ions equally distributed between A and B-sites [5]. $NiFe_2O_4$ exhibit high sensitivity for the reducing gases like chlorine and liquefied petroleum gas [6, 7]. However, to our knowledge the ethanol gas-sensing properties of $NiFe_2O_4$ and Zn doped $NiFe_2O_4$ are still not so widely available.

The gas sensing mechanism involves surface reaction of the oxide surface with the test gas [8]. The ability to control the surface of the nanocrystals by adopting different synthesis routes has opened-up a new dimension to modify material for specific property applications. Also, nano sized materials, which have high surface activity due to their small particle size and enormous surface area, can increase the

efficiency of the chemical sensor [9, 10]. There are several routes to obtain nanosized ferrites such as hydrothermal synthesis, sol-gel, microemulsion techniques, etc.

The aim of the present investigation is to prepare nanocrystalline Zn modified Ni ferrite by citrated sol-gel method with a low calcination temperature involving low cost metal nitrates as raw materials and characterize them for ethanol gas sensing.

2. Experimental details

The stoichiometric molar amounts of Ferric nitrate $[\text{Fe}(\text{NO}_3)_3 \cdot 9\text{H}_2\text{O}]$, Nickel nitrate $[\text{Ni}(\text{NO}_3)_2 \cdot 6\text{H}_2\text{O}]$, Zinc nitrate $[\text{Zn}(\text{NO}_3)_2 \cdot 6\text{H}_2\text{O}]$ and citric acid monohydrate $[\text{C}_6\text{H}_8\text{O}_7 \cdot \text{H}_2\text{O}]$ were weighed and mixed with ethylene glycol. The prepared mixture was stirred magnetically at 80°C for 2 h. A transparent solution was obtained after 2 h. Then, this solution was consequently transferred to Teflon-lined stainless steel autoclave. The temperature of the autoclave was raised slowly to 125°C and maintained for 10 h to get gel precursor. Afterward, the autoclave was allowed to cool naturally to room temperature and the resulting product further heated for 3 h at 350°C in muffle furnace and then milled to a fine powder. The obtained powder was then calcined at 600°C for 5 h to improve the crystallinity of the prepared materials. Fig. 1 shows the flowchart to prepare nanosized $\text{Ni}_{1-x}\text{Zn}_x\text{Fe}_2\text{O}_4$ powder samples.

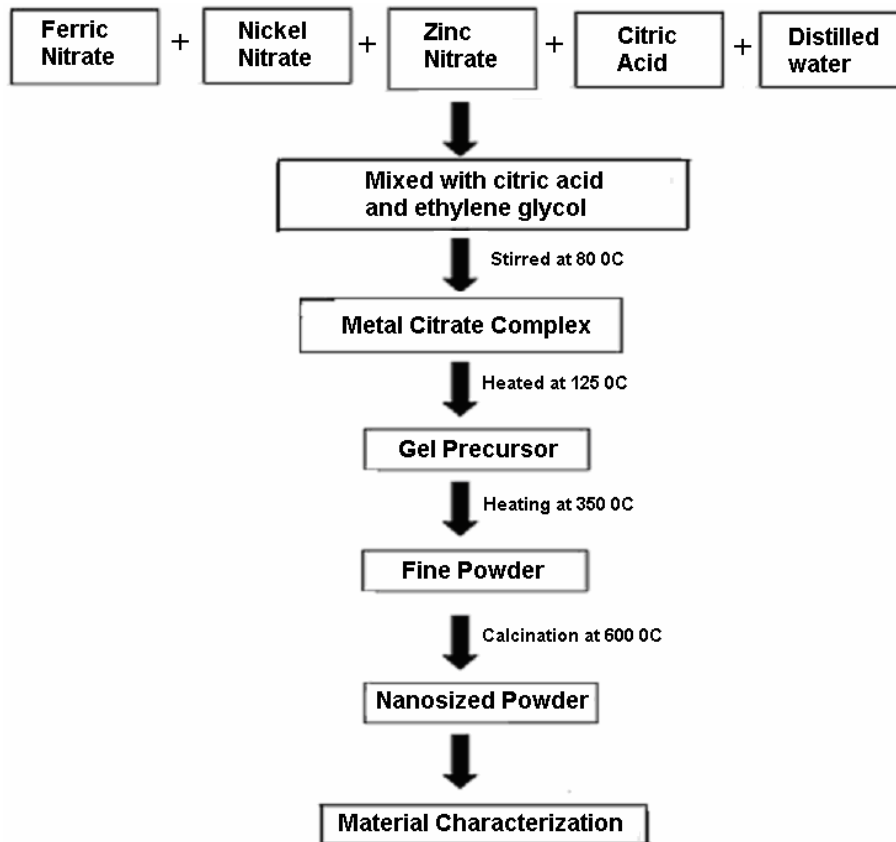


Figure 1. Flow chart for synthesis of $\text{Ni}_{1-x}\text{Zn}_x\text{Fe}_2\text{O}_4$ powders

The structure and constituents of the products were determined on an X-ray diffractometer (Model: Philips X'pert) with a Cu K α radiation ($\lambda = 1.5406\text{\AA}$). The crystallite size (D_{hkl}) of the powder sample was calculated using Scherrer relation, which is given by,

$$D = \frac{K\lambda}{B \cdot \cos\theta}$$

Where B is the full width at half-maximum intensity (in radians) of a peak at an angle θ ; K is a constant, depending on the line shape profile; λ is the wavelength of the X-ray source. The crystallite size was determined by taking the average of the strongest peaks D_{220} , D_{311} , D_{400} , D_{511} and D_{440} .

The description of the sensor fabrication and gas sensing measurements has been already depicted in one of earlier reports [4]. Gas sensing properties were investigated at various operating temperatures from 50 to 350 °C. The experiments were performed with four test gases: liquefied petroleum gas (LPG), ammonia (NH₃), hydrogen (H₂), and ethanol gas (C₂H₅OH). The concentration of test gases was 500 ppm for NH₃, H₂ and LPG whereas it is 100 ppm for C₂H₅OH. The sensor response (S) is defined as the ratio $\Delta R/R_a$, i.e. change in resistance of the sensor (R_a) in air and in the gas (R_g), normalized to the sensor resistance in air.

$$S = \frac{\Delta R}{R_a} = \frac{|R_a - R_g|}{R_a}$$

3. Results and Discussion

3.1. Materials characterizations

The X-ray diffraction patterns of Ni_{1-x}Zn_xFe₂O₄ ($x = 0, 0.2, 0.3$ and 0.4) calcinated at 600 °C are displayed in Fig. 2. The XRD peaks and their positions with the calculated lattice parameters confirm that all the compositions exhibit single-phase cubic spinel structure with Fd3m space group. No peaks corresponding to any additional crystalline component are observed in the obtained patterns. The average crystallite size has been calculated from the XRD peaks using Debye-Scherrer formula and was found in the range of 23-38 nm for all the investigated samples. The lattice parameters estimated from XRD peaks are presented in Table 1. It is observed that the average crystallite size is minimum for Ni_{0.6}Zn_{0.4}Fe₂O₄ composition. Also, it is seen that the lattice parameter increases with an increase of Zn content. The increase in the value of the lattice constant with Zn ion substitution can be explained on the basis of ionic radius, where the ionic radius of Zn ion (0.82 Å) is smaller than that of Ni ion (0.78 Å).

3.2. Ethanol sensing characteristics

To reveal the potential use of the nanocrystalline spinel Ni_{1-x}Zn_xFe₂O₄ ($x = 0, 0.2, 0.3$ and 0.4) synthesized in the present investigation to chemical sensors, its ethanol sensing properties were studied. The response of Ni_{1-x}Zn_xFe₂O₄ to ethanol was measured at different operating temperatures to find out the optimal operating temperature for ethanol detection. The response of the nanocrystalline spinel Ni₁₋

$x\text{Zn}_x\text{Fe}_2\text{O}_4$ to 100 ppm ethanol as a function of operating temperature is illustrated in Fig. 3. It can be seen that the composition $\text{Ni}_{0.6}\text{Zn}_{0.4}\text{Fe}_2\text{O}_4$ exhibited the maximum response to 100 ppm $\text{C}_2\text{H}_5\text{OH}$ at 300 °C. At lower operating temperatures, the sensor response is relatively low, but it increases gradually with an increase in the operating temperature. The sensor response to ethanol attains a maximum at ~300 °C and subsequently it decreases with a further increase of the operating temperature. Thus, the optimal operating temperature for the $\text{Ni}_{0.6}\text{Zn}_{0.4}\text{Fe}_2\text{O}_4$ spinel to detect ethanol was at 300 °C, which is the modest from the perspective of semiconducting oxide gas sensors. Hence, the optimal operating temperature of 300 °C was chosen to investigate further ethanol sensing properties such as response and recovery times, reproducibility and selectivity.

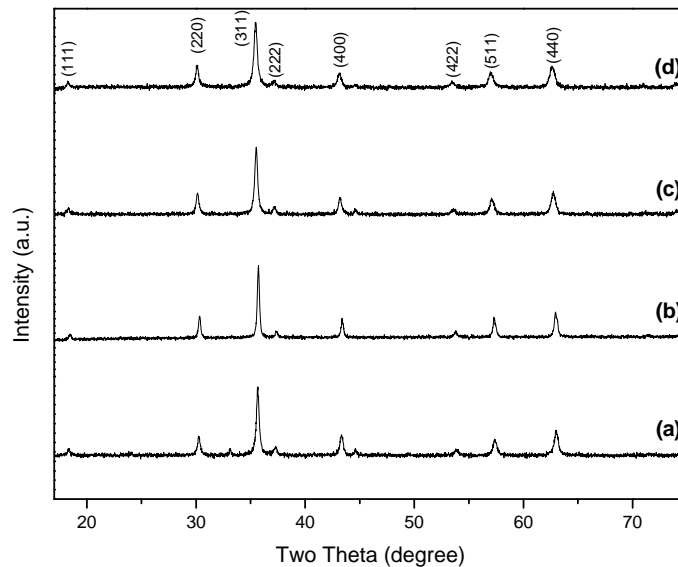


Figure 2. XRD pattern of $\text{Ni}_{1-x}\text{Zn}_x\text{Fe}_2\text{O}_4$ ($x = 0, 0.2, 0.3$ and 0.4) powder samples calcinated at 600 °C.

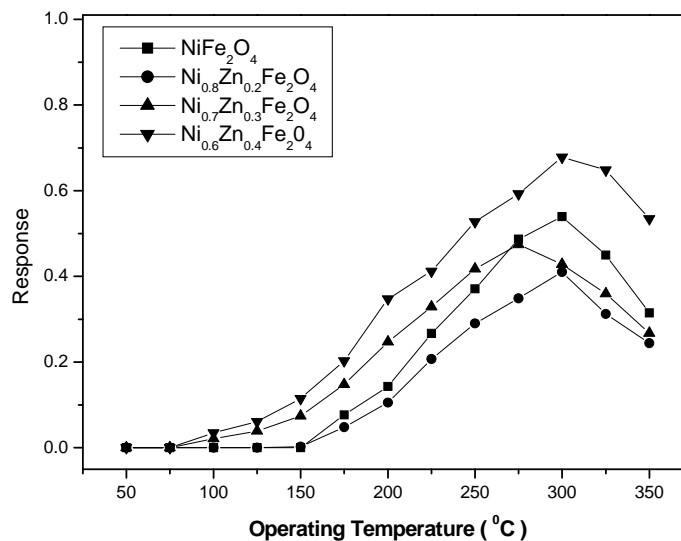


Figure 3. Sensor response of $\text{Ni}_{1-x}\text{Zn}_x\text{Fe}_2\text{O}_4$ ($x = 0, 0.2, 0.3$ and 0.4) to 100 ppm ethanol as a function of operating temperature.

Table 1: Calculated lattice parameters of $\text{Ni}_{1-x}\text{Zn}_x\text{Fe}_2\text{O}_4$ ($x = 0, 0.2, 0.3$ and 0.4)

Sample $\text{Ni}_{1-x}\text{Zn}_x\text{Fe}_2\text{O}_4$	Lattice parameters (Å) $a=b=c$
$x = 0$	8.343 ± 0.002
$x = 0.2$	8.348 ± 0.001
$x = 0.3$	8.379 ± 0.007
$x = 0.4$	8.393 ± 0.002

For practical application of sensor, not only the sensor response but the response and recovery times are also vital parameters for evaluating the performance of gas sensors. The response and recovery times are defined as the time required for the sensor-resistance to change by 90% of the final resistance. It was found that the nanocrystalline $\text{Ni}_{0.6}\text{Zn}_{0.4}\text{Fe}_2\text{O}_4$ based sensor element responds rapidly after introduction of 100 ppm ethanol and recovers immediately when it is exposed to air. The $\text{Ni}_{0.6}\text{Zn}_{0.4}\text{Fe}_2\text{O}_4$ has response time of ~ 70 – 75 s and the recovery time of ~ 180 – 190 s. Furthermore, it was observed that the resistance of the sensing element decreases when exposed to ethanol (reducing gas), which suggests that $\text{Ni}_{0.6}\text{Zn}_{0.4}\text{Fe}_2\text{O}_4$ behaves as a n-type semiconductor.

The variation of the response of nanocrystalline $\text{Ni}_{0.6}\text{Zn}_{0.4}\text{Fe}_2\text{O}_4$ based sensor element with respect to the ethanol concentration at the optimal operating temperature of 300°C is shown in Fig. 4. The $\text{Ni}_{0.6}\text{Zn}_{0.4}\text{Fe}_2\text{O}_4$ spinel is able to detect up to 25 ppm for ethanol with good response at the optimal operating temperature of 300°C .

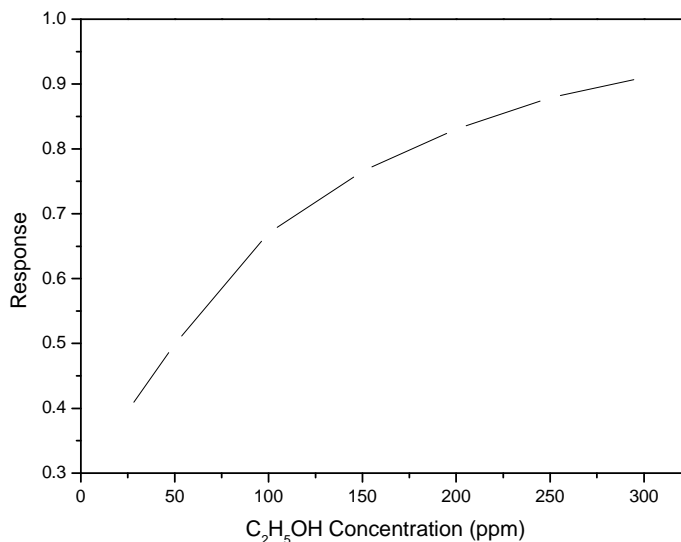


Figure 4. Variation in the response of $\text{Ni}_{0.6}\text{Zn}_{0.4}\text{Fe}_2\text{O}_4$ sensor element at 300°C against ethanol concentration.

Selectivity is an important parameter of gas sensors and the sensor response toward a specific gas needs to be markedly higher than those to other gases for selective gas detection. To study the selective

behavior of the nanocrystalline $\text{Ni}_{0.6}\text{Zn}_{0.4}\text{Fe}_2\text{O}_4$ to ethanol at the optimal operating temperature of $300\text{ }^\circ\text{C}$, the sensor responses towards H_2 , NH_3 and LPG were also measured. The corresponding results are demonstrated in Fig. 5. The $\text{Ni}_{0.6}\text{Zn}_{0.4}\text{Fe}_2\text{O}_4$ exhibits higher response to ethanol, whereas it shows a considerably lower response to H_2 , NH_3 and LPG. Taking into account the results of gas sensing experiments, it is concluded that the nanocrystalline $\text{Ni}_{0.6}\text{Zn}_{0.4}\text{Fe}_2\text{O}_4$ has good ethanol sensing properties such as higher gas response, good selectivity, quick response and recovery, excellent repeatability and relatively lower operating temperature.

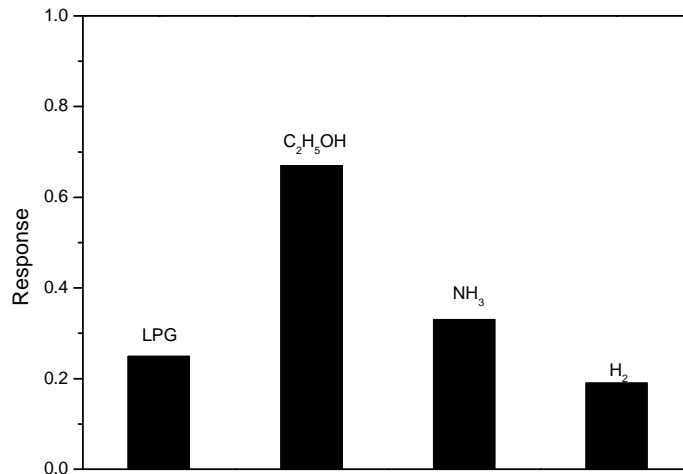
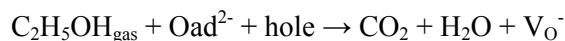
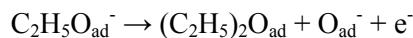
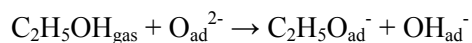


Figure 5. Response of $\text{Ni}_{0.6}\text{Zn}_{0.4}\text{Fe}_2\text{O}_4$ towards 100 ppm $\text{C}_2\text{H}_5\text{OH}$, 500 ppm NH_3 , 500 ppm H_2 and 500 ppm LPG at $300\text{ }^\circ\text{C}$.

3.3. Ethanol sensing mechanism

The oxygen is adsorbed on the surface of the sensor in air and adsorbed oxygen is transformed into chemisorbed oxygen at a definite temperature. The reaction between $\text{C}_2\text{H}_5\text{OH}$ gas and the chemisorbed oxygen ion can take place as [11]:



Where V_{O}^- is a doubly charged oxygen vacancy. These reactions impart electrons into the sensing material, leading to an increase in electron concentration, and a decrease in resistance of the $\text{Ni}_{0.6}\text{Zn}_{0.4}\text{Fe}_2\text{O}_4$ -based sensor.

The concentration of chemisorbed oxygen increased and reached optimum value with the increasing operating temperature. When the absorption-desorption of chemisorbed oxygen attained a dynamic equilibrium, the sensor exhibited maximum response towards ethanol gas at $300\text{ }^\circ\text{C}$. Difference in gas-sensing response to different gases might be due to differences in the adsorption and the reaction processes.

4. Conclusions

In conclusion, $\text{Ni}_{1-x}\text{Zn}_x\text{Fe}_2\text{O}_4$ ($x = 0, 0.2, 0.3$ and 0.4) mixed ferrite powder samples with cubic spinel structure were successfully synthesized by citrate sol-gel route. The response of $\text{Ni}_{0.6}\text{Zn}_{0.4}\text{Fe}_2\text{O}_4$ based sensor element to 100 ppm ethanol was found maximum at an optimal operating temperature 300°C . The response time was $\sim 70\text{--}75$ s and the recovery time was found to be $\sim 180\text{--}190$ s. Furthermore, $\text{Ni}_{0.6}\text{Zn}_{0.4}\text{Fe}_2\text{O}_4$ sensor exhibited good selectivity to $\text{C}_2\text{H}_5\text{OH}$ when operating at 300°C . This means that $\text{Ni}_{0.6}\text{Zn}_{0.4}\text{Fe}_2\text{O}_4$ sensor can be a good candidate for practical application in detecting $\text{C}_2\text{H}_5\text{OH}$ because of the good characteristics mentioned.

Acknowledgement

VDK gratefully acknowledges the financial assistance from the University Grants Commission (U.G.C.), New Delhi, India through the Minor Research Project No. F. 47-762/13(WRO).

References

- [1] R.D. McMichael, R.D. Shull, L.J. Swartzendruber, L.H. Bennett, R.E. Watson, *J. Magn. Magn. Mater.*, 1992, **111**, 29-33.
- [2] C.V. Gopal Reddy, S.V. Manorama, V.J. Rao, *J. Mater. Sci. Lett.*, 2000, **9**, 775-778.
- [3] Y.-L. Liu, Z.-M. Liu, Y. Yang, H.F. Yang, G.-L. Shen, R.-Q. Yu, *Sens. Actuators B*, 2005, **107**, 600-604.
- [4] V. D. Kapse, S. A. Ghosh, F. C. Raghuvanshi and S. D. Kapse, *Mater. Chem. Phys.*, 2009, **113**, 638–644.
- [5] C.N. Chinnasamy, A. Narayanasamy, N. Ponpandian, K. Chattopadhyay, K. Shinoda, B. Jeyadevan, *Phys. Rev. B*, 2001, **63**, 184108–184116.
- [6] R.C.V. Gopal, S.V. Manorama, V.J. Rao, *Sensor. Actuat. B* 1999, **55**, 90–95.
- [7] L. Satyanarayana, R.K. Madhusudan, S.V. Manorama, *Mater. Chem. Phys.*, 2003, **82**, 21–26.
- [8] M.J. Madou, S.R. Morrison, *Chemical Sensing in Solid State Devices*, Academic Press, San Diago, 1989.
- [9] K.N.P. Kumar, K. Keizer, A.J. Burggraaf, T. Okubo, H. Nagamoto, S. Morooka, *Nature*, 1992, **358**, 48–51.
- [10] G. Sberveglieri, L.E. Depero, M. Ferroni, V. Guidi, G. Martinelli, P. Nelli, C. Perego, L. Sangletti, *Adv. Mater.*, 1996, **8**, 334-337.
- [11] Z.P. Sun, L. Liu, D.Z. Jia, W.Y. Pan, *Sens. Actuators B*, 2007, **125**, 144-148.